Published in final edited form as:
Neurobiol Aging. 2008 July ; 29(7): 1080–1092. doi:10.1016/j.neurobiolaging.2007.01.014.

The role of mtDNA mutations in the pathogenesis of age-related hearing loss in mice carrying a mutator DNA polymerase γ

Shinichi Someya[a,b], **Tatsuya Yamasoba**[c], **Gregory C. Kujoth**[a], **Thomas D. Pugh**[d], **Richard Weindruch**[d], **Masaru Tanokura**[b], and **Tomas A. Prolla**[a,*]

[a]Departments of Genetics & Medical Genetics, University of Wisconsin, Madison, WI 53706, USA

[b]Department of Applied Biological Chemistry, University of Tokyo, Tokyo 113-8657, Japan

[c]Department of Otolaryngology, University of Tokyo, Tokyo 113-8655, Japan

[d]Department of Medicine and Veterans Administration Hospital, University of Wisconsin, Madison, WI 53705, USA

Abstract

Mitochondrial DNA (mtDNA) mutations may contribute to aging and age-related diseases. Previously, we reported that accumulation of mtDNA mutations is associated with age-related hearing loss in mice carrying a mutator allele of the mitochondrial *Polg* DNA polymerase. To elucidate the role of mtDNA mutations in the pathogenesis of age-related hearing loss or presbycusis, we performed large scale gene expression analysis to identify mtDNA mutation-responsive genes and biological process categories associated with mtDNA mutations by comparing the gene expression patterns of cochlear tissues from 9-month-old mitochondrial mutator and control mice. mtDNA mutations were associated with transcriptional alterations consistent with impairment of energy metabolism, induction of apoptosis, cytoskeletal dysfunction, and hearing dysfunction in the cochlea of aged mitochondrial mutator mice. TUNEL staining and caspase-3 immunostaining analysis demonstrated that the levels of apoptotic markers were significantly increased in the cochleae of mitochondrial mutator mice compared to age-matched controls. These observations support a new model of how mtDNA mutations impact cochlear function whereby accumulation of mtDNA mutations lead to mitochondrial dysfunction, an associated impairment of energy metabolism, and the induction of an apoptotic program. The data presented here provide the first global assessment at the molecular level of the pathogenesis of age-related disease in mitochondrial mutator mice and reveal previously unrecognized biological pathways associated with mtDNA mutations.

Keywords

mtDNA mutations; *Polg*; Age-related hearing loss; Presbycusis; Apoptosis; Mitochondrial dysfunction; Aging

*Corresponding author at: Departments of Genetics & Medical Genetics, University of Wisconsin, 425-G Henry Mall, Madison, WI 53706, USA. Tel.: +1 608 265 5204; fax: +1 608 262 2976. taprolla@wisc.edu (T.A. Prolla).

Conflict of interest
The authors declare no actual or potential conflicts of interest.

1. Introduction

The mitochondrial theory of aging postulates that reactive oxygen species (ROS) generated inside mitochondria damage key mitochondrial components such as mtDNA, membranes, and respiratory chain proteins (Balaban et al., 2005). Such damage accumulates with time, leads to age-related mitochondrial dysfunction, and causes energy depletion, compromising the organism. Mitochondria are the main source of cellular energy, generating most cellular ATP. The mammalian mitochondrial genome consists of 37 genes, encoding 13 proteins of the electron transport oxidative phosphorylation system (Anderson et al., 1981). Since mtDNA plays an essential role in energy metabolism, mtDNA mutations have been hypothesized to contribute to mammalian aging. Indeed, previous studies have shown that mtDNA point mutations accumulate with aging in humans (Michikawa et al., 1999), and that accumulation of mtDNA mutations leads to premature aging in mitochondrial mutator mice, indicating a causal role of mtDNA mutations in mammalian aging (Kujoth et al., 2005; Trifunovic et al., 2004).

Specific mutations in mtDNA have also been implicated in the development of age-related diseases (Corral-Debrinski et al., 1992; Dirks et al., 2006; Seidman et al., 2002). Age-related hearing loss, also known as presbycusis, is one of the most common diseases of aging and the number of people affected is rapidly growing as the elderly population increases. However, the pathogenesis of age-related hearing loss remains unclear. The accumulation of mtDNA mutations has been associated with the development of age-related hearing loss (Kujoth et al., 2005). In support of this hypothesis, hearing loss is a common symptom in individuals harboring inherited mtDNA mutations (Chinnery et al., 2000). Several mutations in *Polg* (mitochondrial DNA polymerase gamma) have been identified as a cause of human disorders such as Alpers syndrome and deafness (Mancuso et al., 2004; Nguyen et al., 2005). Specific mtDNA point mutations also contribute to mitochondrial disorders in humans such as mitochondrial encephalomyopathy, lactic acidosis and stroke-like episodes (MELAS) and myoclonic epilepsy and ragged red fibres (MERRF), the symptoms of which include hearing loss (Chinnery et al., 2000; Fischel-Ghodsian, 2003). Furthermore, more than 100 different deletions of mtDNA have been associated with mitochondrial disorders (Chinnery et al., 2000), and of these, some mtDNA deletions cause Kearns–Sayre syndrome which also involves hearing loss (Chinnery et al., 2000).

We have shown previously that mtDNA mutations play a role in the development of age-related hearing loss in mice carrying a mutation in *Polg* (Kujoth et al., 2005). These mice were created by introducing a two base substitution, which results in a critical residue substitution in the exonuclease domain of *Polg*, impairing its mtDNA proof-reading ability (Kujoth et al., 2005). These animals accumulate mtDNA mutations with aging, and exhibit a striking premature aging phenotype, consisting of osteoporosis, reduced lifespan, and hearing loss (Kujoth et al., 2005; Trifunovic et al., 2004). Thus, these mice represent a useful model for investigating a role of mtDNA mutations in the pathogenesis of age-related hearing loss. In the present study, we performed genome-wide DNA microarray analysis using cochlear tissues from 9-month-old mitochondrial mutator and control mice. We then performed data analysis to identify age-related, mtDNA mutation-responsive genes and

biological process categories statistically associated with mtDNA mutation-responsive genes. Quantitative RT-PCR (QRT-PCR), TUNEL staining, immunostaining, histology, and hearing assessment were performed to corroborate the microarray results. Together, these approaches revealed previously unrecognized biological process pathways associated with mtDNA mutations, providing a new model of how mtDNA mutations impact cochlear function.

2. Materials and methods

2.1. Animals

Polg$^{D257A/D257A}$ mice have been previously described and were backcrossed four generations onto the C57BL/6 background (Kujoth et al., 2005). Mice were housed in the Genetics and Biotechnology Center of University of Wisconsin-Madison-approved Animal Care Facility. Experiments were performed in accordance with the protocols approved by the University of Wisconsin Institutional Animal Care and Use Committee (Madison, WI).

2.2. Assessment of hearing

Detailed protocols for ABR measurements have been described (Someya et al., 2007). Briefly, ABRs were measured with a tone burst stimulus (4, 8, and 16 kHz) using an ABR recording system (Intelligent Hearing System, Miami, FL). Mice were anesthetized with a mixture of xylazine hydrochloride (10 mg/kg, i.m.) and ketamine hydrochloride (40 mg/kg, i.m.). We used five mice per group for this study. Following the hearing measurements, the same mice were sacrificed to conduct microarray analysis of cochlear gene expression. Data were analyzed using the two-tailed standard *t*-test. All data were reported as mean ± S.E.M.

2.3. Assessment of histology

Detailed protocols for tissue processing have been described (Sakamoto et al., 2004). Briefly, 4% paraformaldehyde-fixed and paraffin-embedded specimens were sliced into 4μm sections, mounted on silane-coated slides, stained with Haematoxylin and Eosin (HE), and observed under a light microscope (Leica Microsystems, Bannockburn, IL). The Rosenthal's canal was divided into three regions: apical, middle and basal (Keithley et al., 2004) and the apical and basal turns were used for evaluation of cochlear histology. We used five mice for each group ($n = 5$) that were different mice than those used in the microarray analysis. Five modiolar sections obtained in every fifth section from one unilateral cochlea were evaluated per mouse. The same animals were used for spiral ganglion cell counting, TUNEL staining, and immunostaining.

Spiral ganglion cells (SGCs) were counted in the apical turn of the cochlear sections in the field of 0.3 μm ± 0.225 μm as seen using a 40 × objective by direct observation. SGCs were identified by the presence of a nucleus. The SGC density was calculated as the number of SGCs per 1mm^2. Five sections of the unilateral apical turn were evaluated in one cochlea per mouse. Data were analyzed using the two-tailed standard *t*-test. All data were reported as mean ± S.E.M.

2.4. RNA sample preparations

Detailed protocols for gene expression profiling analysis using Affymetrix microarrays by Affymetrix algorithms have been described (Affymetrix, 2004; Lee et al., 1999). Briefly, we pooled two cochleae from each mouse for one sample because the amount of mRNA from one cochlea of one mouse was insufficient for a single GeneChip (Affymetrix, Santa Clara, CA).We hybridized each sample to a single GeneChip and used five samples per group.

2.5. Statistical analysis

Signals in each image were scaled to a whole chip target intensity of 1500 using GeneChip® Operating Software (GCOS) 1.3 in order to minimize an overall variability in hybridization intensities. A gene probe set was considered “expressed” if it displayed a “present” call in at least one GeneChip based on the Affymetrix “present/absent call” algorithms. All genes considered “not expressed” were eliminated from our analysis. Further analysis and comparisons between the two groups were also done using GCOS 1.3 and Significance Analysis of Microarray (SAM) (Tusher et al., 2001). To identify mtDNA-responsive genes, each 9-monthold WT sample ($n = 5$) was compared to each 9-month-old D257A sample ($n = 5$), generating a total of 25 pairwise comparisons. The change in gene expression was considered significant if the fold change was >1.0 based on the Affymetrix algorithms (Affymetrix, 2004), the *P*-value was <0.02 using the two-tailed standard *t*-test, and FDR was <10% based on the SAM algorithms (Tusher et al., 2001). We then used Database for Annotation, Visualization, and Integrated Discovery (DAVID) (Dennis et al., 2003) and Expression Analysis Systematic Explorer (EASE) (Hosack et al., 2003) (http://apps1.niaid.nih.gov/david/) to assign identified genes to “Gene Ontology (GO): Biological Process” categories of Gene Ontology Consortium (www.geneontology.org) and used EASE to determine the total number of identified genes that were assigned to each biological process category, the total number of genes on the array in each biological process category, and to identify “GO: Biological Process” categories statistically associated with mtDNA mutation-responsive genes by performing Fisher Exact tests (Fisher Exact score < 0.05). Five genes were manually assigned to “perception of sound” category using the gene list of “Hereditary Hearing Impairment in Mice” by The Jackson Laboratory (http://www.jax.org/hmr/master_table.html). The complete set of microarray data has been submitted to the GEO (Gene Expression Omnibus) repository (http://www.ncbi.nlm.nih.gov/geo/) with GEO Accession number GSE4866. For further details of the methods (MIAME checklist), see Supplementary information (Supplementary note).

2.6. Quantitative RT-PCR

Detailed protocols for QRT-PCR analysis have been described (Someya et al., in press). Detection of mRNA was carried out with the TaqMan EZ RT-PCR kit using the Applied Biosystems Prism 7000 Sequence Detection System (Applied Biosystems, Foster City, CA). Oligonucleotide primers and MGB fluorescent probes (TaqMan Gene Expression Assays) were purchased from Applied Biosystems. Each sample used for QRT-PCR analysis

Appendix A. Supplementary data

Supplementary information associated with this article can be found, in the online version, at doi:10.1016/j.neurobiolaging.2007.01.014.

consisted of the two cochleae pooled from one mouse. We used four mice per group ($n = 4$) for this study. mRNA samples used for QRT-PCR analysis were from different mice than those used for microarray analysis which had been exhausted for that purpose. All data were reported as mean ± S.E.M.

2.7. TUNEL staining

Detailed protocols for TUNEL staining have been described (Someya et al., 2007). Briefly, TUNEL staining for apoptotic nuclei was performed using the DeadEnd Colorimetric TUNEL System (Promega, Madison, WI) according to the manufacturer's instructions. Briefly, stained sections were viewed by light microscopy and spiral ganglions in the apical turns were evaluated for TUNEL positivity. We used five mice for each group ($n = 5$) that were different mice than those used in the microarray analysis, but the same as those used for spiral ganglion cell counting and immunostaining. Data were evaluated using the two-tailed standard *t*-test. All data were reported as mean ± S.E.M.

2.8. Immunostaining

Detailed protocols for immunohistochemical staining have been described (Someya et al., 2007). Immunohistochemical staining for caspase-3 was performed using the Anti-Active Caspase-3 pAb (Promega, Madison, WI) according to the manufacturer's instructions. Briefly, positively-stained cells were observed in sections of the cochleae by direct observation using a light microscopy. Spiral ganglions in the apical turns were evaluated for caspase-3 positivity. We used five mice for each group ($n = 5$) that were different mice than those used in the microarray analysis, but the same as those used for spiral ganglion cell counting and TUNEL staining. Data were evaluated using the two-tailed standard *t*-test. All data were reported as mean ± S.E.M.

3. Results

3.1. Assessment of hearing and histology

The C57BL/6 strain possesses mutations in the Cdh23 gene which result in onset of age-related hearing loss and cochlear degeneration beginning at 8–10 months (Keithley et al., 2004; Noben-Trauth et al., 2003). Because the background of our mice is C57BL/6 and both $Polg^{D257A/D257A}$ (D257A) and $Polg^{+/+}$ wild-type (WT) mice possess the mutations, we first evaluated hearing function of 8–9-month-old WT mice and confirmed that they did not show any age-related hearing loss at the frequencies examined under the housing conditions of our animal facility. We then chose to study 9-month-old WT mice and age-matched D257A mice, an age at which WT mice do not have hearing loss due to the *Cdh23* mutations.

To determine whether D257A mice display age-related hearing loss, we measured auditory brainstem response (ABR) thresholds in 9-month-old WT and D257A mice. Nine-month-old WT mice displayed normal hearing. However, the age-matched D257A mice displayed significant age-related hearing loss ($P < 0.05$, n=5) (Fig. 1). To confirm whether D257A mice display age-related cochlear degeneration, we performed histological examination of the cochleae from 2- and 9-month-old WT and D257A mice ($n = 5$). Examination of the histology of the apical cochlear region confirmed that two of the five cochleae from 9-

month-old D257A mice displayed severe loss of SGCs (Fig. 2J and L). Consistent with our previous studies, all the cochleae from 9-month-old D257A mice displayed severe loss of SGCs in the basal turn (Fig. 3G) (Kujoth et al., 2005). In contrast, all the cochleae from 2-month-old WT and D257A mice displayed no or only a few loss of SGCs (Fig. 2A, C, D, and F). The five cochleae from 9-month-old WT mice also displayed no clear loss of SGCs (Fig. 2G and I). Decreased SGC density is one of the hallmarks of presbycusis in mammals (Keithley et al., 2004). The mean SGC density of 9-month-old D257A mice was significantly lower than that of age-matched WT (Fig. 2M) ($P < 0.05$, $n = 5$). There was no significant difference in the SGC density between 2-monthold WT, age-matched D257A, and 9-month-old WT mice (Fig. 2M). Hair cell loss is another hallmark of presbycusis (Francis et al., 2003). Examination of the histology of the basal cochlear region confirmed that two of the five cochleae from 9-month-old D257A mice displayed severe loss of outer hail cells (OHCs) and inner hair cells (IHCs) (Fig. 3G and H), whereas all the cochleae from 2-month-old WT and D257A and 9-month-old WT mice displayed no or only a few loss of the OHCs and IHCs (Fig. 3A–F). All the cochleae from 2- and 9-month-old WT and D257A mice also displayed no or only a few loss of the OHCs and IHCs in the apical cochlear region (Fig. 2B, E, H, and K). Together, these observations confirm that D257A mice display age-related hearing loss and cochlear degenerations by 9 months of age.

3.2. Overview of microarray and statistical analysis

To identify mtDNA mutation-responsive genes and associated biological process categories, we conducted genome-wide gene expression analysis using RNA samples isolated from cochlear tissues of 9-month-old WT and D257A mice ($n = 5$). We selected cochlear tissue for our investigation because the cochlea is primarily composed of long-lived, high oxygen-consuming postmitotic cells (Pickles, 2004), a feature shared with other critical postmitotic tissues such as heart and brain which are sites of multiple, major age-related diseases and show accumulation of mtDNA mutations (Corral-Debrinski et al., 1992). We used the Affymetrix mouse genome 430 2.0 array, which contains 45,037 gene probe sets representing more than 34,000 mouse genes and ESTs. We then performed statistical analysis using the Affymetrix algorithms (Affymetrix, 2004), SAM algorithms (Tusher et al., 2001), and our own data analysis criteria. We found that 1289 gene probe sets were significantly up-regulated, and 662 gene probe sets were significantly down-regulated in cochlear tissues from 9-month-old D257A mice. The gene probe sets were further assigned to “GO: Biological Process” categories of the Gene Ontology Consortium using DAVID (Dennis et al., 2003), resulting in classification of 466 up-regulated and 378 down-regulated genes. Gene probe sets were considered “genes” if they had been assigned a “gene symbol” annotation by DAVID. We then used EASE (Hosack et al., 2003) to determine the number of identified genes and the total number of genes on the array in each biological process category, and to test the statistical significance of coregulation (overrepresentation) of identified genes within each biological process category. For this analysis, we used the Fisher Exact test ($P < 0.05$), whose score represents the probability that an overrepresentation of a certain biological process category occurs by random chance (Hosack et al., 2003). A summary of the Gene Ontology Biological Process categories statistically associated with mtDNA-responsive genes is shown in Table 1. A list of selected

genes altered in expression is shown in Table 2. For all genes identified, see Supplementary information (Table 3).

3.3. mtDNA mutations result in up-regulation of genes involved in apoptosis and stress response

EASE analysis revealed that two apoptotic process categories, “regulation of apoptosis” and “anti-apoptosis”, were significantly associated with the mtDNA mutation-responsive genes (Fisher Exact score < 0.05), and 15 genes within these categories were significantly up-regulated in the cochleae ($P < 0.02$, false discover rate (FDR) < 10%) (Table 1). Of the 15 genes identified, 10 genes were involved in regulation of apoptosis, including phosphatase and tensin homolog (*Pten*), BCL2-like 11 (apoptosis facilitator) (*Bim*), baculoviral IAP repeat-containing 6 (*Birc6*), and beta-amyloid binding protein precursor (*Bbp*) (Table 2). *Bim* is a member of the proapoptotic Bcl2 family and a well-described component of mitochondrial apoptosis pathway, leading to cytochrome *c* release (Cheng et al., 2001; Putcha et al., 2001). *Birc6* is also involved in mitochondrial pathways of apoptosis (Ren et al., 2005). Phosphatase and tensin homolog is a tumor suppressor phosphatase that regulates Akt kinase activity and may promote apoptotic death of hippocampal neurons (Gary and Mattson, 2002). The EASE analysis also revealed that 13 genes in the “programmed cell death” category were up-regulated, including serum/glucocorticoid regulated kinase (*Sgk*), programmed cell death 6 interacting protein (*Pdcd6ip*), and tumor necrosis factor receptor superfamily, member 1a (*Tnfrsf1a*) ($P < 0.02$, FDR < 10%, Fisher Exact score = 0.21) (Table 2). *Sgk* is a member of a serine/threonine kinase family and is involved in the early pathogenesis of Parkinson’s disease (Schoenebeck et al., 2005). The protein encoded by *Pdcd6ip* regulates neuronal death involving caspase pathways (Trioulier et al., 2004). *Tnfrsf1a* is a member of a TNFR superfamily and is involved in activation of Bid, a Bcl-2 family member and inducer of mitochondrial pathways of apoptosis (Yin, 2000). QRT-PCR analysis was conducted for *Pten* and *Bim*, to validate the microarray results for expression of these genes. The QRT-PCR results were in agreement with the microarray findings that expression of these proapoptotic genes were increased in the cochlea of D257A mice (Fig. 4).

Proteolysis also plays a key role in cell death (Hengartner, 2000). The EASE analysis revealed that 14 genes involved in the “proteolysis and peptidolysis” category were found to be up-regulated, including a disintegrin-like and metalloprotease (reprolysin type) with thrombospondin type 1 motif, 4 (*Adamts4*), a disintegrin and metalloproteinase domain 15 (metargidin) (*Adam15*), and cathepsin G (*Ctsg*) ($P < 0.02$, FDR < 10%, Fisher Exact score = 0.88) (Table 2). The proteins encoded by *Adamts4* and *Adam15* are involved in proteolysis of neurocan, aggrecan, and versican, members of a proteoglycan family, and components of the extracellular matrix in various tissues (Gao et al., 2002). Cathepsins are cysteine proteases that are released from lysosomes and play a key role in apoptotic cell death (Chwieralski et al., 2006). Up-regulation of these proteolysis genes provides further evidence of increased transcriptional apoptotic activity in the aging cochlea (Table 2).

Stress responses may trigger apoptotic cell death (Mattson, 2000). The EASE analysis revealed that 15 genes involved in the “response to stress” category were up-regulated,

including heat shock protein 1 (*Hspb1*) and myeloperoxidase (*Mpo*) ($P < 0.02$, FDR < 10%, Fisher Exact score = 0.65) (Table 2). The generation of ROS plays an important role in immune-mediated defense against infection, tumor cells, and cell damage (Aratani et al., 1999). Myeloperoxidase produces hypochlorous acid from hydrogen peroxide and chloride, and plays a key role in microbial killing or immune-mediated cell destruction (Aratani et al., 1999). In the mammalian brain, small heat shock proteins are induced in response to physiological stress such as tissue injury (Murashov et al., 1998). *Hspb1* is a member of the small heat shock protein family and has been characterized as a molecular chaperone required for protection of motor neurons under conditions of stress (Murashov et al., 1998). Together, these results provide evidence that mtDNA mutations result in significant up-regulation of genes involved in multiple apoptotic and stress pathways in the cochlea of aged mitochondrial mutator mice.

3.4. mtDNA mutations result in down-regulation of genes involved in energy metabolism

The EASE analysis revealed that one of the key energy metabolism categories, “carbohydrate metabolism”, was significantly suppressed in D257A mice (Fisher Exact score < 0.05), and that 13 genes in this category were significantly down-regulated in the cochlea ($P < 0.02$, FDR < 10%) (Table 1). These include phosphorylase kinase alpha 1 (*Phka1*), phosphoglucomutase 2-like 1 (*Pgm2l1*), and phosphorylase kinase gamma 1 (*Phkg1*) (Table 2). The glycogen phosphorylase kinases such as phosphorylase kinase alpha 1 and phosphorylase kinase gamma 1 are key enzymes involved in glycogen metabolism and regulate glycogen breakdown by activating glycogen phosphorylase (Wuyts et al., 2005). *Pgm2l1* is a member of a Phosphoglucomutase gene family involved in glycolysis and gluconeogenesis (Levin et al., 1999). Phosphoglucomutases regulate the interconversion of glucose 1-phosphate and glucose 6-phosphate in the glycolysis pathway (Levin et al., 1999). The EASE analysis also revealed that 13 genes in the “mitochondrion” category were down-regulated, including aquaporin 1 (*Aqp1*), PERP, TP53 apoptosis effector (*Perp*), and hydroxyacyl-Coenzyme A dehydrogenase/3-ketoacyl-Coenzyme A thiolase/enoyl-Coenzyme A hydratase (trifunctional protein), beta subunit (*Hadhb*) ($P < 0.02$, FDR < 10%, Fisher Exact score = 0.79) (Table 2). Aquaporins are membrane proteins that regulate water transport. Specific members of this water channel family have been shown to be expressed in the mitochondria of mammalian brain (Amiry-Moghaddam et al., 2005). Aquaporin 1, a member of the water channel family is localized in the stria vascularis of rat cochlea and is thought to play a key role in ion transport of the auditory system (Sawada et al., 2003). The protein encoded by *Hadhb* is a subunit of a multienzyme complex or mitochondrial functional protein that is involved in mitochondrial μ-oxidation (Orii et al., 1997). QRT-PCR analysis was conducted for *Eno3* and *Acsm3* from these energy metabolism categories (Table 2), to validate the microarray results for expression of these genes. Aconsistent agreement between the two methods was observed (Fig. 4). Together, these observations provide evidence that mtDNA mutations result in down-regulation of genes involved in energy metabolism in the cochlea of aged mitochondrial mutator mice, consistent with mitochondrial dysfunction and associated impairment of energy metabolism.

3.5. mtDNA mutations result in down-regulation of genes involved in cytoskeletal regulation

The EASE analysis revealed that six cytoskeletal regulation categories, including "cytoskeleton", "extracellular matrix", "collagen", "structural molecule activity", "myosin", and "cell adhesion", were significantly suppressed in D257A mice (Fisher Exact score < 0.05), and that 132 genes in these categories were significantly down-regulated as a result of age-related accumulation of mtDNA mutations ($P < 0.02$, FDR < 10%) (Table 1). Of the 132 genes identified, 39 genes were associated with the "cytoskeleton" category, including 5 myosin encoding genes: *Myl1*, *Myh1*, *Myl2*, *Myh2*, and *Mylpf* (Table 2). Myosins are a family of actin-based molecular motor proteins and play an important role in the auditory system (Gillespie, 2002). For example, the protein encoded by *Myo7a* is localized along the actin-rich stereocilia of hair cells in the cochlea (Gillespie, 2002; Wolfrum et al., 1998). Further, specific mutations in *myo7a*, *myo15*, and *myo6* are associated with deafness (Kros et al., 2002; Melchionda et al., 2001). Twenty-five genes in the "extracellular matrix" category were significantly downregulated, including eight collagen encoding genes: *Col3a1*, *Col1a2*, *Col5a2*, *Col4a1*, *Col17a1*, *Col15a1*, and *Col6a3* (Table 2). Type IX collagen is thought to play a key structural role in the tectorial membrane of the organ of Corti in cochlea (Suzuki et al., 2005). Specific mutations in *Col1a1*, *Col4a3*, *Col4a4*, *Col4a5*, and *Col11a2* cause conductive hearing loss in humans (Chen et al., 2005; Gratton et al., 2005; Iliadou et al., 2006). The EASE analysis also revealed that 22 genes in the "cell adhesion" category were significantly down-regulated, including cadherin 13 (*Cdh13*) (Table 2), a member of a cadherin family that mediates cell–cell adhesion or cell-extracellular matrix interactions (Zheng et al., 2005). Specific mutations in *Cdh23* and *Pcdh15* cause hearing loss in mice (Noben-Trauth et al., 2003; Zheng et al., 2005). QRT-PCR analysis was conducted for *Col17a1*, to validate the microarray results for expression of these genes. A consistent agreement between the two methods was observed (Fig. 4). These results provide evidence that mtDNA mutations result in down-regulation of genes involved in cytoskeletal regulation in the cochlea of aged mitochondrial mutator mice, consistent with cytoskeletal dysfunction.

3.6. mtDNA mutations result in down-regulation of genes associated with hearing function

Gene expression profiling revealed that six genes involved in the "perception of sound" category were down-regulated, including procollagen, type I, alpha 1 (*Col1a1*) and otogelin (*Otog*) ($P < 0.02$, FDR < 10%) (Table 2). Otosclerosis, a bony dystrophy of the otic capsule caused by abnormal resorption and redeposition of bony tissue, is one of the common causes of hearing loss (Rodriguez et al., 2004). Hearing loss in this disease most commonly results from the fixation of the stapedial footplate to the oval window, which prevents ossicular vibration in response to sound (Rodriguez et al., 2004). Specific mutations in *Col1a1* have been associated with this disorder (Rodriguez et al., 2004). The Otog gene encodes otogelin, an *N*-glycosylated protein, which is thought to play a key role in the deflection of the stereocilia bundles in the hair cells of the cochlea (Simmler et al., 2000). Specific mutations in this gene also cause deafness (Simmler et al., 2000).

In the cochlea, ion transport is needed to maintain proper ionic balance essential for hearing function (Jespersen et al., 2005). The EASE analysis revealed that 12 genes in the "ion

transport" category were down-regulated, including gamma-aminobutyric acid (GABA-A) receptor, subunit alpha 1 (*Gabra1*), glutamate receptor, ionotropic, AMPA2 (alpha 2) (*Gria2*), and potassium voltage-gated channel, shaker-related, subfamily, member 6 (*Kcna6*) ($P < 0.02$, FDR < 10%, Fisher Exact score = 0.79) (Table 2). The protein encoded by *Gabra1* is a receptor subunit for gamma-aminobutyric acid (GABA), a major inhibitory neurotransmitter in mammalian brain (Ma et al., 2005; Rosmond et al., 2002). *Gria2* encodes a glutamate receptor subunit that is involved in glutamatergic transmission (Mead and Stephens, 2003). QRT-PCR analysis was conducted for *Col1a1*, to validate the microarray results for expression of these genes. A consistent agreement between the two methods was observed (Fig. 4). These observations were consistent with the ABR findings, and together provide evidence that mtDNA mutations result in down-regulation of genes involved in hearing function in the cochlea of aged mitochondrial mutator mice.

3.7. TUNEL staining and immunostaining

Apoptosis results in nuclear DNA fragmentation (Rich et al., 2000). To confirm whether levels of apoptosis are increased in the cochleae of aged D257A mice, we performed the TUNEL staining to examine cochleae from 2-and 9-month-old WT and D257A mice. We selected spiral ganglion cells in the apical region for evaluation of TUNEL staining because spiral ganglion cells were severely degenerated in the basal region of 9-month-old D257A mice. The mean percentage of TUNEL-positive cells in 9-month-old D257A mice (4.1%) was significantly elevated compared to those of 2-month-old WT (0.8%) and D257A (1.0%), and 9-month-old WT mice (1.5%) ($P < 0.05$, $n = 5$) (Fig. 5A–E).

An additional indicator of apoptotic cell death is the activation of caspases (Hengartner, 2000; Yuan and Yankner, 2000). To examine whether levels of activated caspase-3 are increased in the cochleae of aged D257A mice, we examined cochleae of 2- and 9-month-old WT and D257A mice by immunostaining using an antibody for cleaved caspase-3. We also selected spiral ganglion cells in the apical region for this study. The mean percentage of cleaved caspase-3-positive cells in 9-month-old D257A mice (3.7%) was significantly elevated compared to that seen in 2-monthold WT (0.5%) and D257A (0.7%), and 9-month-old WT mice (1.2%) ($P < 0.05$, n=5) (Fig. 6A–E). These results were consistent with the microarray findings, and together provide evidence that mtDNA mutations result in induction of apoptosis in the cochlea of aged mitochondrial mutator mice.

4. Discussion

The data presented here provide the first comprehensive gene expression analysis of a tissue in aged mitochondrial mutator mice and reveal previously unreported pathways associated with age-related hearing loss that may provide insights into pathogenic mechanisms. It has been postulated that mitochondrial function declines with aging partly due to oxidative damage to mtDNA, and that the resulting mitochondrial dysfunction leads to impairment of energy metabolism. Indeed, mitochondrial ATP content and production has been shown to decline with aging in the rat muscle by ~50% (Dirks et al., 2006). Mitochondrial ATP production also declines with advancing aging in human skeletal muscle (Short et al., 2005). Furthermore, mitochondrial mutator mice display a decline in respiratory enzyme activities

and mitochondrial ATP production rates with aging in the heart, suggesting a role of mtDNA mutations as a cause of energy metabolism impairment (Trifunovic et al., 2004). In the present study, we observed transcriptional evidence for a decline in carbohydrate metabolism and mitochondrial function in the cochlea of aged mitochondrial mutator mice, suggesting that accumulation of mtDNA mutations leads to energy metabolism impairment. We have shown previously that the frequency of mtDNA mutations in the cytochrome *b* gene region from 5-month-old D257A mice was ~3–8 times that in the age-matched WT mice for heart, liver, and duodenum (Kujoth et al., 2005). An independent group has also reported that the frequency of somatic mtDNA point mutations in the cytochrome *b* gene region from 8-week-old mitochondrial mutator mice was approximately ~5 times higher than that of the age-matched wild-type mice for brain, and that further increases at 25 weeks were not significant (Trifunovic et al., 2004). These reports suggest that although a substantial load of mtDNA mutations may be present by 2 months of age in the cochlea of D257A mice, it takes several more months to develop age-related hearing loss in these animals. We did not measure the frequency of mtDNA mutations in the cochlear tissue of D257A mice, but similar to all other tissues examined in this model, it is likely that these mice have a substantial burden of mtDNA mutations in this tissue. With aging, this may lead to mitochondrial dysfunction, resulting in impairment of energy metabolism.

A progressive decline in mitochondrial function and associated energy depletion in aging muscle have been associated with sarcopenia, an age-related loss of muscle mass and strength (Dirks et al., 2006). It has been postulated that apoptosis induced by mitochondrial dysfunction and associated impairment of energy metabolism in aged muscle tissue may contribute to the development of sarcopenia (Dirks et al., 2006). Indeed, impairment of respiratory function is associated with induction of apoptosis (Dirks et al., 2006; Kujoth et al., 2005). We have previously reported that aged mitochondrial mutator mice display an increase in the levels of apoptotic markers in liver, testes, thymus, intestine, and muscle (Kujoth et al., 2005). Furthermore, Parkinson’s disease disease, one of the well-known age-related neuronal diseases, has also been associated with apoptotic death of neurons and mitochondrial mutations (Mattson, 2000). Interestingly, caloric restriction, known to retard aging and age-related diseases, has shown to suppress apoptotic cell death in the mouse cochlea and prevents age-related hearing loss (Someya et al., 2007), implicating apoptosis in the development of age-related hearing loss. In the present study, we observed up-regulation of over 50 genes associated with apoptotic pathways and a marked increase in the levels of apoptotic markers in the aging cochlea. Because D257A mice have a substantial burden of mtDNA mutations in postmitotic tissues, it is possible that these mtDNA mutations lead to mitochondrial dysfunction and associated impairment of energy metabolism, resulting in activation of apoptosis. Together, our observations and these cited reports suggest that apoptosis may play a major role in the pathogenesis of age-related hearing loss in mammals, and that mtDNA mutations is likely to induce apoptotic cell death in the mammalian cochlea.

Structural proteins such as myosins, collagens, and cadherins play a key role in maintaining the structural integrity and motor activity of cochlear cells and mediating the cell-to-cell interaction essential for auditory function (Gillespie, 2002; Suzuki et al., 2005; Zheng et al.,

2005). Indeed, defects or mutations in a number of myosin, collagen, and cadherin genes have been associated with hearing loss (Chen et al., 2005; Gratton et al., 2005; Iliadou et al., 2006; Kros et al., 2002; Melchionda et al., 2001; Noben-Trauth et al., 2003; Zheng et al., 2005). Of these mutations, *Cdh23* mutations have been linked to age-related hearing loss in mice and humans (Noben-Trauth et al., 2003). Cadherin 23 is specifically expressed in the stereocillia of the hair cells in the cochlea and plays a key role in perception of sound (Noben-Trauth et al., 2003). The C57BL/6 strain, a mouse homozygous for the *Cdh23* mutation, has increased susceptibility to early onset of presbycusis (Zheng and Johnson, 2001), indicating that this modifier gene plays a key role in its pathogenesis. It is possible that mtDNA mutations may lead to accelerating cochlear degeneration due to the Cdh23 mutations in the C57BL/6 background. Furthermore, it is likely that several other modifier genes contribute to presbycusis and our microarray observations raise the possibility that these unknown modifiers might include genes involved in cytoskeletal regulation identified herein. We note that a dramatic down-regulation of the expression of Myh2 (fold change = −136.0), Lmod2 (−38.2), and Col17a1 (−14.0) genes was observed, implicating these genes as potential candidates for modifier or marker genes of age-related hearing loss. We also observed severe loss of spiral ganglion neurons and down-regulation of over one hundred genes involved in cytoskeletal regulation in D257A mice. Because impaired energy metabolism can lead to apoptosis, it is possible that loss of critical cells such as spiral ganglion neurons due to apoptosis may cause damage to the structural proteins of cochlea, resulting in cytoskeletal dysfunction. Together, our observations suggest that cytoskeletal dysfunction may be a key feature of age-related hearing loss.

Our findings suggest a previously unreported model of how mtDNA mutations impact cochlear function (Fig. 7). In this model, *Polg* infidelity causes accumulation of mtDNA mutations, leading to mitochondrial dysfunction and associated impairment of energy metabolism. The energy depletion in turn induces apoptosis, leading to loss of critical cochlear cells such as hair cells and spiral ganglion neurons. These processes eventually cause loss of cochlear function, resulting in age-related hearing loss. The relevance of this model to human presbycusis, mitochondrial diseases, and aging in general is worthy of further exploration.

Acknowledgments

We thank S. Kinoshita and Y. Kurasawa for histological processing. This research was supported by NIH grants AG021905 (T.A.P.), AG18922 (R.W.), MEXT grant (the National Project on Protein Structural and Functional Analyses) (M.T.), MHLW grants 15110201 (T.Y), 13470357 (T.Y. and M.T.).

References

Affymetrix. Expression Analysis Technical Manual. Santa Clara, CA: Affymetrix; 2004.

Amiry-Moghaddam M, Lindland H, Zelenin S, Roberg BA, Gundersen BB, Petersen P, Rinvik E, Torgner IA, Ottersen OP. Brain mitochondria contain aquaporin water channels: evidence for the expression of a short aqp9 isoform in the inner mitochondrial membrane. FASEB J. 2005; 19:1459–1467. [PubMed: 16126913]

Anderson S, Bankier AT, Barrell BG, de Bruijn MH, Coulson AR, Drouin J, Eperon IC, Nierlich DP, Roe BA, Sanger F, Schreier PH, Smith AJ, Staden R, Young IG. Sequence and organization of the human mitochondrial genome. Nature. 1981; 290:457–465. [PubMed: 7219534]

Aratani Y, Koyama H, Nyui S, Suzuki K, Kura F, Maeda N. Severe impairment in early host defense against candida albicans in mice deficient in myeloperoxidase. Infect. Immun. 1999; 67:1828–1836. [PubMed: 10085024]

Balaban RS, Nemoto S, Finkel T. Mitochondria, oxidants, and aging. Cell. 2005; 120:483–495. [PubMed: 15734681]

Chen W, Kahrizi K, Meyer NC, Riazalhosseini Y, Van Camp G, Najmabadi H, Smith RJ. Mutation of col11a2 causes auto-somal recessive non-syndromic hearing loss at the dfnb53 locus. J. Med. Genet. 2005; 42:e61. [PubMed: 16033917]

Cheng EH, Wei MC, Weiler S, Flavell RA, Mak TW, Lindsten T, Korsmeyer SJ. Bcl-2, bcl-x(l) sequester bh3 domain-only molecules preventing bax- and bak-mediated mitochondrial apoptosis. Mol. Cell. 2001; 8:705–711. [PubMed: 11583631]

Chinnery PF, Elliott C, Green GR, Rees A, Coulthard A, Turnbull DM, Griffiths TD. The spectrum of hearing loss due to mitochondrial DNA defects. Brain. 2000; 123((Pt 1)):82–92. [PubMed: 10611123]

Chwieralski CE, Welte T, Buhling F. Cathepsin-regulated apoptosis. Apoptosis. 2006; 11:143–149. [PubMed: 16502253]

Corral-Debrinski M, Horton T, Lott MT, Shoffner JM, Beal MF, Wallace DC. Mitochondrial DNA deletions in human brain: regional variability and increase with advanced age. Nat. Genet. 1992; 2:324–329. [PubMed: 1303288]

Dennis G Jr, Sherman BT, Hosack DA, Yang J, Gao W, Lane HC, Lempicki RA. David: Database for annotation, visualization, and integrated discovery. Genome Biol. 2003; 4:P3. [PubMed: 12734009]

Dirks AJ, Hofer T, Marzetti E, Pahor M, Leeuwenburgh C. Mitochondrial DNA mutations, energy metabolism and apoptosis in aging muscle. Ageing Res. Rev. 2006; 5:179–195. [PubMed: 16647308]

Fischel-Ghodsian N. Mitochondrial deafness. Ear Hear. 2003; 24:303–313. [PubMed: 12923421]

Francis HW, Ryugo DK, Gorelikow MJ, Prosen CA, May BJ. The functional age of hearing loss in a mouse model of presbycusis. II. Neuroanatomical correlates. Hear Res. 2003; 183:29–36. [PubMed: 13679135]

Gao G, Westling J, Thompson VP, Howell TD, Gottschall PE, Sandy JD. Activation of the proteolytic activity of adamts4 (aggrecanase-1) by c-terminal truncation. J. Biol. Chem. 2002; 277:11034–11041. [PubMed: 11796708]

Gary DS, Mattson MP. Pten regulates akt kinase activity in hippocampal neurons and increases their sensitivity to glutamate and apoptosis. Neuromol. Med. 2002; 2:261–269.

Gillespie PG. Myosin-viia and transduction channel tension. Nat. Neurosci. 2002; 5:3–4. [PubMed: 11753408]

Gratton MA, Rao VH, Meehan DT, Askew C, Cosgrove D. Matrix metalloproteinase dysregulation in the stria vascularis of mice with alport syndrome: implications for capillary basement membrane pathology. Am. J. Pathol. 2005; 166:1465–1474. [PubMed: 15855646]

Hengartner MO. The biochemistry of apoptosis. Nature. 2000; 407:770–776. [PubMed: 11048727]

Hosack DA, Dennis G Jr, Sherman BT, Lane HC, Lempicki RA. Identifying biological themes within lists of genes with ease. Genome Biol. 2003; 4:R70. [PubMed: 14519205]

Iliadou V, Van Den Bogaert K, Eleftheriades N, Aperis G, Vanderstraeten K, Fransen E, Thys M, Grigoriadou M, Pampanos A, Economides J, Iliades T, Van Camp G, Petersen MB. Monogenic nonsyndromic otosclerosis: audiological and linkage analysis in a large greek pedigree. Int. J. Pediatr. Otorhinolaryngol. 2006; 70:631–637. [PubMed: 16168495]

Jespersen T, Grunnet M, Olesen SP. The kcnq1 potassium channel: from gene to physiological function. Physiology (Bethesda). 2005; 20:408–416. [PubMed: 16287990]

Keithley EM, Canto C, Zheng QY, Fischel-Ghodsian N, Johnson KR. Age-related hearing loss and the ahl locus in mice. Hear Res. 2004; 188:21–28. [PubMed: 14759567]

Kros CJ, Marcotti W, van Netten SM, Self TJ, Libby RT, Brown SD, Richardson GP, Steel KP. Reduced climbing and increased slipping adaptation in cochlear hair cells of mice with myo7a mutations. Nat. Neurosci. 2002; 5:41–47. [PubMed: 11753415]

Kujoth GC, Hiona A, Pugh TD, Someya S, Panzer K, Wohlgemuth SE, Hofer T, Seo AY, Sullivan R, Jobling WA, Morrow JD, Van Remmen H, Sedivy JM, Yamasoba T, Tanokura M, Weindruch R, Leeuwenburgh C, Prolla TA. Mitochondrial DNA mutations, oxidative stress, and apoptosis in mammalian aging. Science. 2005; 309:481–484. [PubMed: 16020738]

Lee CK, Klopp RG, Weindruch R, Prolla TA. Gene expression profile of aging and its retardation by caloric restriction. Science. 1999; 285:1390–1393. [PubMed: 10464095]

Levin S, Almo SC, Satir BH. Functional diversity of the phosphoglucomutase superfamily: structural implications. Protein Eng. 1999; 12:737–746. [PubMed: 10506283]

Ma DQ, Whitehead PL, Menold MM, Martin ER, Ashley-Koch AE, Mei H, Ritchie MD, Delong GR, Abramson RK, Wright HH, Cuccaro ML, Hussman JP, Gilbert JR, Pericak-Vance MA. Identification of significant association and gene–gene interaction of gaba receptor subunit genes in autism. Am. J. Hum. Genet. 2005; 77:377–388. [PubMed: 16080114]

Mancuso M, Filosto M, Bellan M, Liguori R, Montagna P, Baruzzi A, DiMauro S, Carelli V. Polg mutations causing ophthalmoplegia, sensorimotor polyneuropathy, ataxia, and deafness. Neurology. 2004; 62:316–318. [PubMed: 14745080]

Mattson MP. Apoptosis in neurodegenerative disorders. Nat. Rev. Mol. Cell Biol. 2000; 1:120–129. [PubMed: 11253364]

Mead AN, Stephens DN. Involvement of ampa receptor glur2 subunits in stimulus-reward learning: Evidence from glutamate receptor gria2 knock-out mice. J. Neurosci. 2003; 23:9500–9507. [PubMed: 14573529]

Melchionda S, Ahituv N, Bisceglia L, Sobe T, Glaser F, Rabionet R, Arbones ML, Notarangelo A, Di Iorio E, Carella M, Zelante L, Estivill X, Avraham KB, Gasparini P. Myo6, the human homologue of the gene responsible for deafness in snell's waltzer mice, is mutated in autosomal dominant nonsyndromic hearing loss. Am. J. Hum. Genet. 2001; 69:635–640. [PubMed: 11468689]

Michikawa Y, Mazzucchelli F, Bresolin N, Scarlato G, Attardi G. Aging-dependent large accumulation of point mutations in the human mtdna control region for replication. Science. 1999; 286:774–779. [PubMed: 10531063]

Murashov AK, Talebian S, Wolgemuth DJ. Role of heat shock protein hsp25 in the response of the orofacial nuclei motor system to physiological stress. Brain. Res. Mol. Brain Res. 1998; 63:14–24. [PubMed: 9838025]

Nguyen KV, Ostergaard E, Ravn SH, Balslev T, Danielsen ER, Vardag A, McKiernan PJ, Gray G, Naviaux RK. Polg mutations in alpers syndrome. Neurology. 2005; 65:1493–1495. [PubMed: 16177225]

Noben-Trauth K, Zheng QY, Johnson KR. Association of cadherin 23 with polygenic inheritance and genetic modification of sensorineural hearing loss. Nat. Genet. 2003; 35:21–23. [PubMed: 12910270]

Orii KE, Aoyama T, Wakui K, Fukushima Y, Miyajima H, Yamaguchi S, Orii T, Kondo N, Hashimoto T. Genomic and mutational analysis of the mitochondrial trifunctional protein beta-subunit (hadhb) gene in patients with trifunctional protein deficiency. Hum. Mol. Genet. 1997; 6:1215–1224. [PubMed: 9259266]

Pickles JO. Mutation in mitochondrial DNA as a cause of presbyacusis. Audiol. Neurootol. 2004; 9:23–33. [PubMed: 14676471]

Putcha GV, Moulder KL, Golden JP, Bouillet P, Adams JA, Strasser A, Johnson EM. Induction of bim, a proapoptotic bh3-only bcl-2 family member, is critical for neuronal apoptosis. Neuron. 2001; 29:615–628. [PubMed: 11301022]

Ren J, Shi M, Liu R, Yang QH, Johnson T, Skarnes WC, Du C. The birc6 (bruce) gene regulates p53 and the mitochondrial pathway of apoptosis and is essential for mouse embryonic development. Proc. Natl. Acad. Sci. U.S.A. 2005; 102:565–570. [PubMed: 15640352]

Rich T, Allen RL, Wyllie AH. Defying death after DNA damage. Nature. 2000; 407:777–783. [PubMed: 11048728]

Rodriguez L, Rodriguez S, Hermida J, Frade C, Sande E, Visedo G, Martin C, Zapata C. Proposed association between the col1a1 and col1a2 genes and otosclerosis is not supported by a case-control study in spain. Am. J. Med. Genet. A. 2004; 128:19–22. [PubMed: 15211650]

Rosmond R, Bouchard C, Bjorntorp P. Allelic variants in the gaba(a)alpha6 receptor subunit gene (gabra6) is associated with abdominal obesity and cortisol secretion. Int. J. Obes. Relat. Metab. Disord. 2002; 26:938–941. [PubMed: 12080446]

Sakamoto T, Kondo K, Yamasoba T, Suzuki M, Sugasawa M, Kaga K. Overexpression of erbb-2 protein in human middle ear cholesteatomas. Laryngoscope. 2004; 114:1988–1991. [PubMed: 15510028]

Sawada S, Takeda T, Kitano H, Takeuchi S, Okada T, Ando M, Suzuki M, Kakigi A. Aquaporin-1 (aqp1) is expressed in the stria vascularis of rat cochlea. Hear Res. 2003; 181:15–19. [PubMed: 12855358]

Schoenebeck B, Bader V, Zhu XR, Schmitz B, Lubbert H, Stichel CC. Sgk1, a cell survival response in neurodegenerative diseases. Mol. Cell Neurosci. 2005; 30:249–264. [PubMed: 16125969]

Seidman MD, Ahmad N, Bai U. Molecular mechanisms of age-related hearing loss. Ageing Res. Rev. 2002; 1:331–343. [PubMed: 12067590]

Short KR, Bigelow ML, Kahl J, Singh R, Coenen-Schimke J, Raghavakaimal S, Nair KS. Decline in skeletal muscle mitochondrial function with aging in humans. Proc. Natl. Acad. Sci. U.S.A. 2005; 102:5618–5623. [PubMed: 15800038]

Simmler MC, Cohen-Salmon M, El-Amraoui A, Guillaud L, Benichou JC, Petit C, Panthier JJ. Targeted disruption of otog results in deafness and severe imbalance. Nat. Genet. 2000; 24:139–143. [PubMed: 10655058]

Someya S, Yamasoba T, Weindruch R, Prolla TA, Tanokura M. Caloric restriction suppresses apoptotic cell death in the mammalian cochlea and leads to prevention of presbycusis. Neurobiol. Aging. 2007; 28:1613–1622. [PubMed: 16890326]

Suzuki N, Asamura K, Kikuchi Y, Takumi Y, Abe S, Imamura Y, Hayashi T, Aszodi A, Fassler R, Usami S. Type ix collagen knock-out mouse shows progressive hearing loss. Neurosci. Res. 2005; 51:293–298. [PubMed: 15710493]

Trifunovic A, Wredenberg A, Falkenberg M, Spelbrink JN, Rovio AT, Bruder CE, Bohlooly YM, Gidlof S, Oldfors A, Wibom R, Tornell J, Jacobs HT, Larsson NG. Premature ageing in mice expressing defective mitochondrial DNA polymerase. Nature. 2004; 429:417–423. [PubMed: 15164064]

Trioulier Y, Torch S, Blot B, Cristina N, Chatellard-Causse C, Verna JM, Sadoul R. Alix, a protein regulating endosomal trafficking, is involved in neuronal death. J. Biol. Chem. 2004; 279:2046–2052. [PubMed: 14585841]

Tusher VG, Tibshirani R, Chu G. Significance analysis of microar-rays applied to the ionizing radiation response. Proc. Natl. Acad. Sci. U.S.A. 2001; 98:5116–5121. [PubMed: 11309499]

Wolfrum U, Liu X, Schmitt A, Udovichenko IP, Williams DS. Myosin viia as a common component of cilia and microvilli. Cell Motil. Cytoskeleton. 1998; 40:261–271. [PubMed: 9678669]

Wuyts W, Reyniers E, Ceuterick C, Storm K, de Barsy T, Martin JJ. Myopathy and phosphorylase kinase deficiency caused by a mutation in the phka1 gene. Am. J. Med. Genet. A. 2005; 133:82–84. [PubMed: 15637709]

Yin XM. Bid, a critical mediator for apoptosis induced by the activation of fas/tnf-r1 death receptors in hepatocytes. J. Mol. Med. 2000; 78:203–211. [PubMed: 10933582]

Yuan J, Yankner BA. Apoptosis in the nervous system. Nature. 2000; 407:802–809. [PubMed: 11048732]

Zheng QY, Johnson KR. Hearing loss associated with the modifier of deaf waddler (mdfw) locus corresponds with age-related hearing loss in 12 inbred strains of mice. Hear Res. 2001; 154:45–53. [PubMed: 11423214]

Zheng QY, Yan D, Ouyang XM, Du LL, Yu H, Chang B, Johnson KR, Liu XZ. Digenic inheritance of deafness caused by mutations in genes encoding cadherin 23 and protocadherin 15 in mice and humans. Hum. Mol. Genet. 2005; 14:103–111. [PubMed: 15537665]

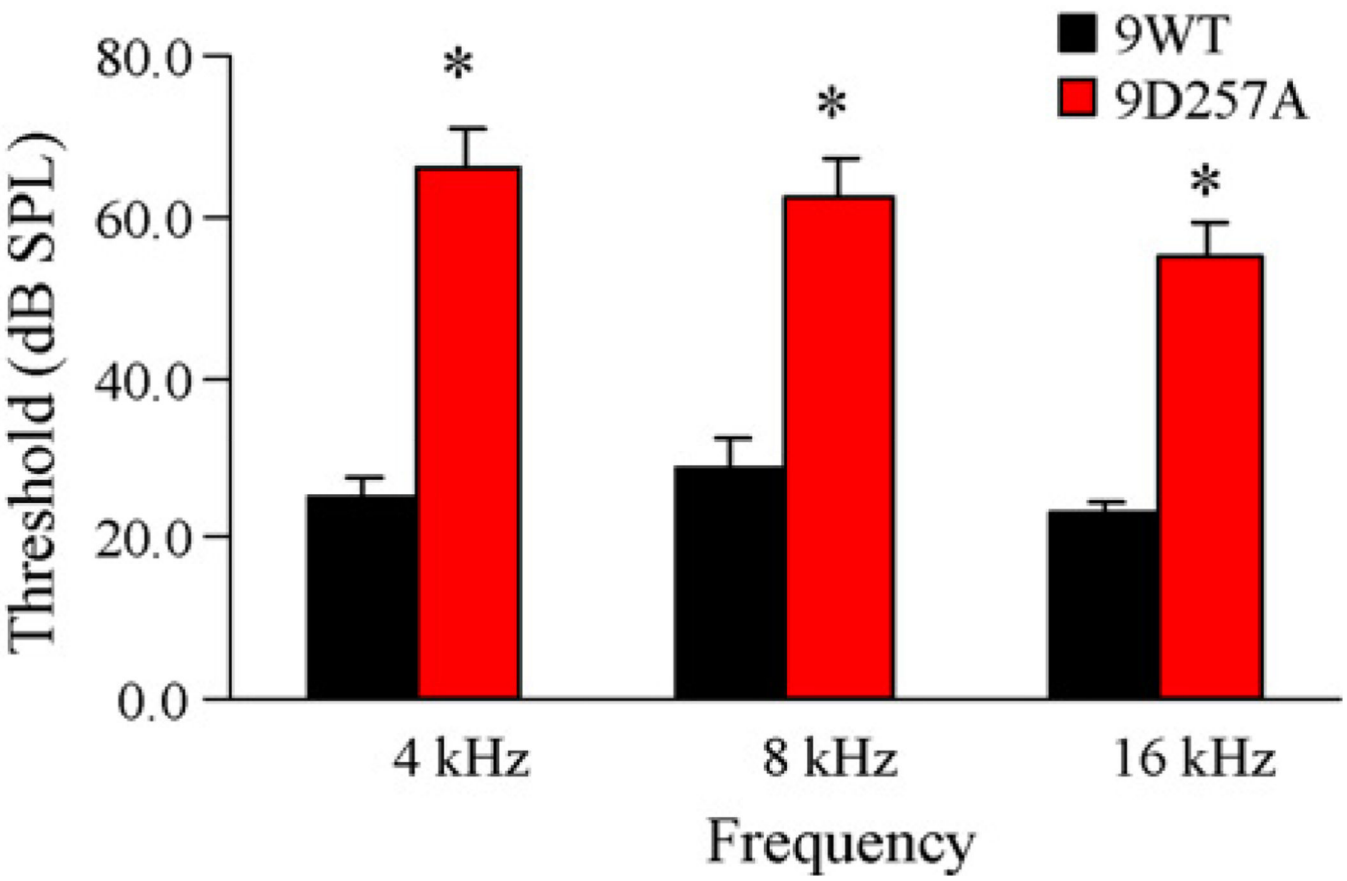

Fig. 1.

Age-related hearing loss. Means of ABR thresholds (dB SPL, decibels sound pressure level) for 9-month-old WT and D257A mice at 4, 8, and 16 kHz. The mean ABR thresholds of 9-month-old D257A mice were significantly elevated compared to the age-matched WT mice (*$P < 0.05$, $n = 5$), showing age-related hearing loss. Error bars represent S.E.M.

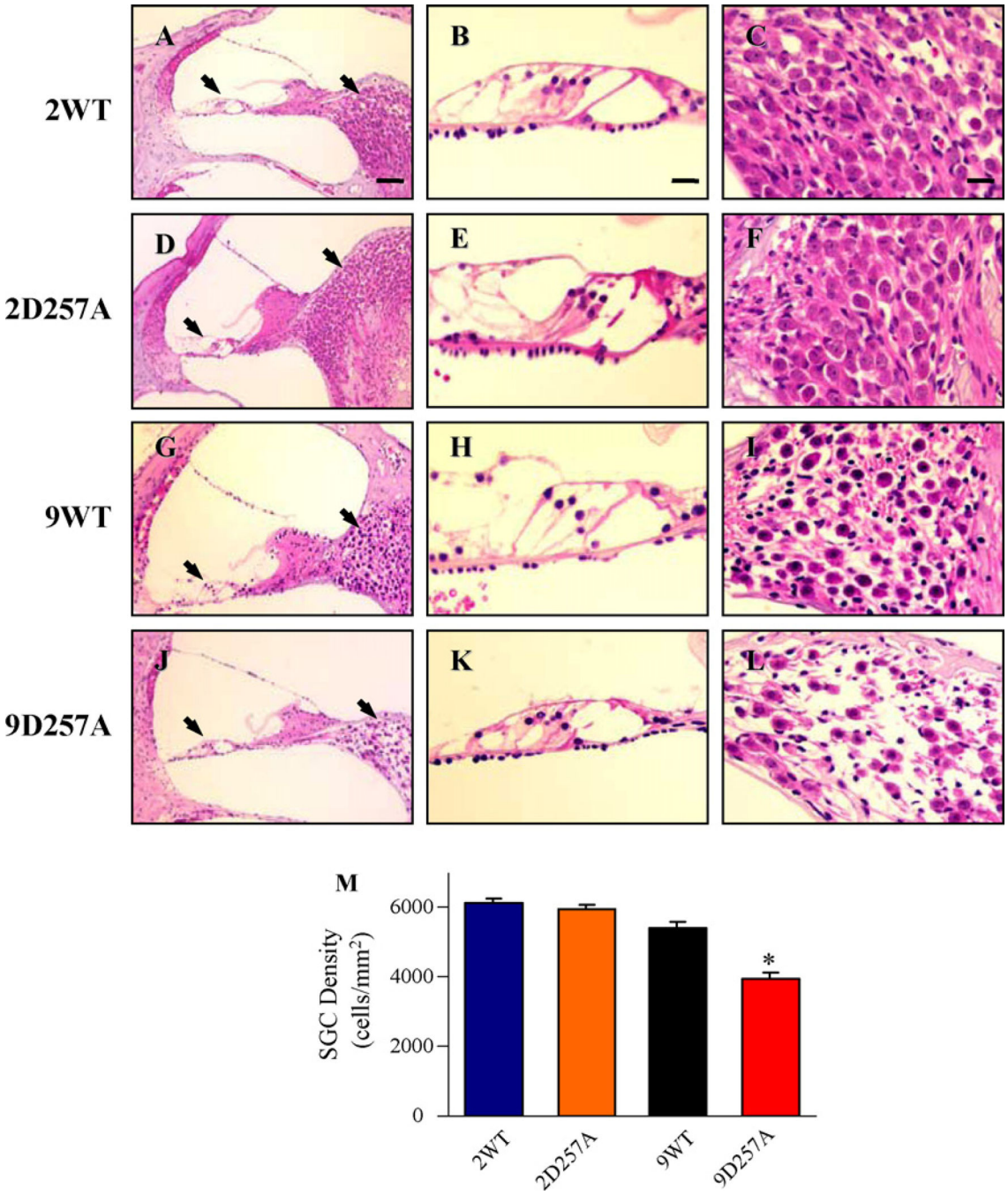

Fig. 2.

Age-related cochlear degeneration. Cochlear apical turn from 2-month-old WT (A–C) and D257A (D–F), and 9-month-old WT (G–I) and D257A (J–L) mice. Arrows indicate hair cells and spiral ganglion cells (SGCs). The cochleae from 2-month-old WT and D257A, and 9-month-old WT mice displayed no or only a few loss of the hair cells and spiral SGCs, whereas the cochleae from 9-month-old D257A mice displayed severe loss of SGCs. The mean SGC density of D257A mice was significantly lower than that of age-matched WT

(M) (*$P < 0.05$, $n = 5$). Error bars represent S.E.M. Scale bar = 100μm (left panel). Scale bar = 25μm (middle and right panel).

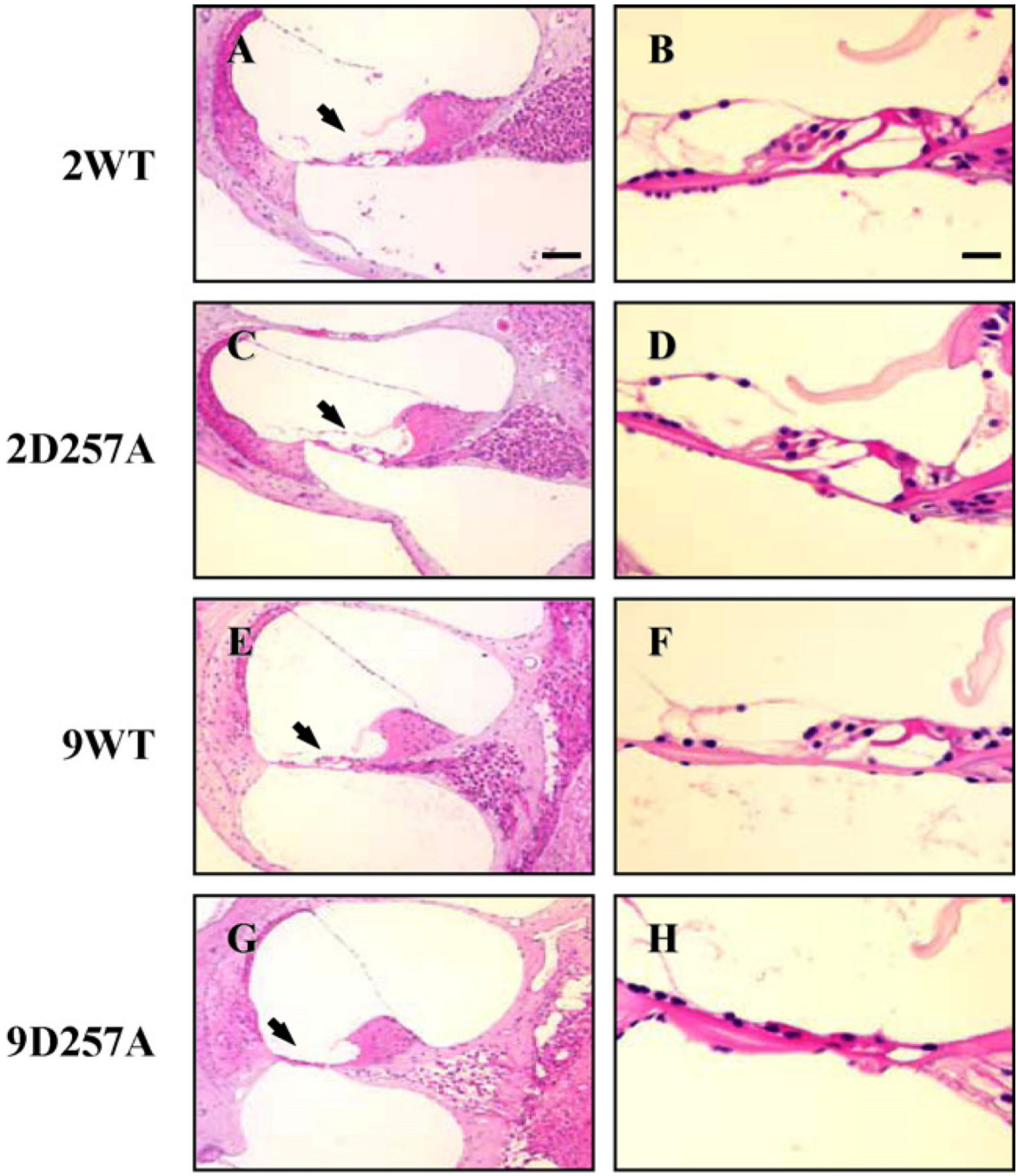

Fig. 3.

Age-related hair cell loss. Cochlear basal turn from 2-month-oldWT (A and B) and D257A (C and D), and 9-month-oldWT(E and F) and D257A (G and H) mice. Arrows indicate hair cells. The cochleae from 9-month-old D257A mice displayed severe loss of the out hair cells (OHCs) and inner hair cells (IHCs), whereas the cochleae from 2-month-old WT and D257A, and 9-month-old WT mice displayed no or only a few loss of the OHCs and IHCs. Scale bar = 100μm (left panel). Scale bar = 25μm (right panel).

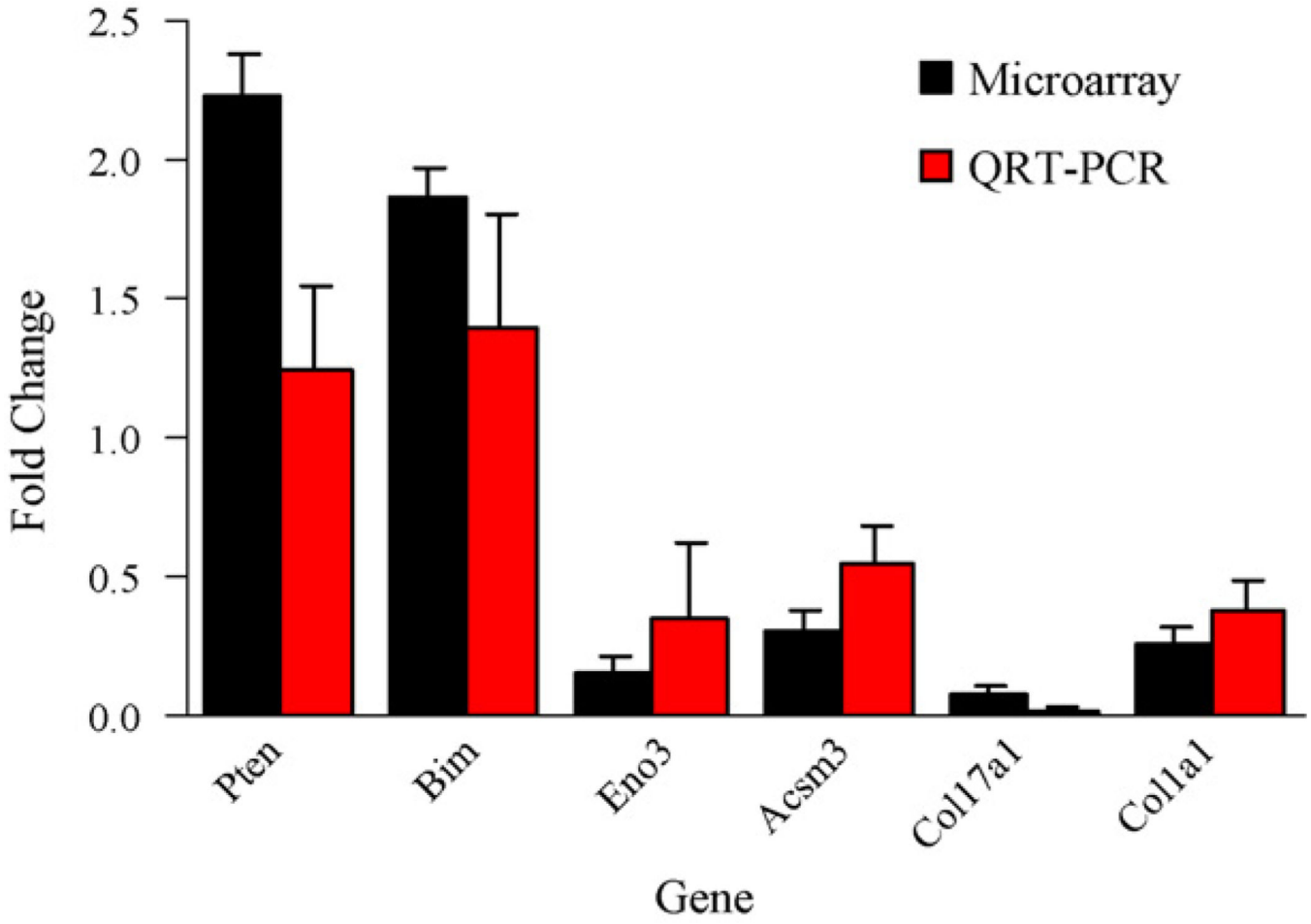

Fig. 4.

QRT-PCR validation of microarray data. The data represent the fold-change in gene expression of 9-month-old D257A cochlea compared to age-matched WT based on average signal intensities of microarray hybridizations (n = 4) and gene expression levels determined by quantitative RT-PCR (n = 4). A consistent agreement between fold-change determined by the two methods was observed. Error bars represent SEM. Fold change: 9-month-old WT to age-matched D257A ratio. QRT-PCR: quantitative RTPCR.

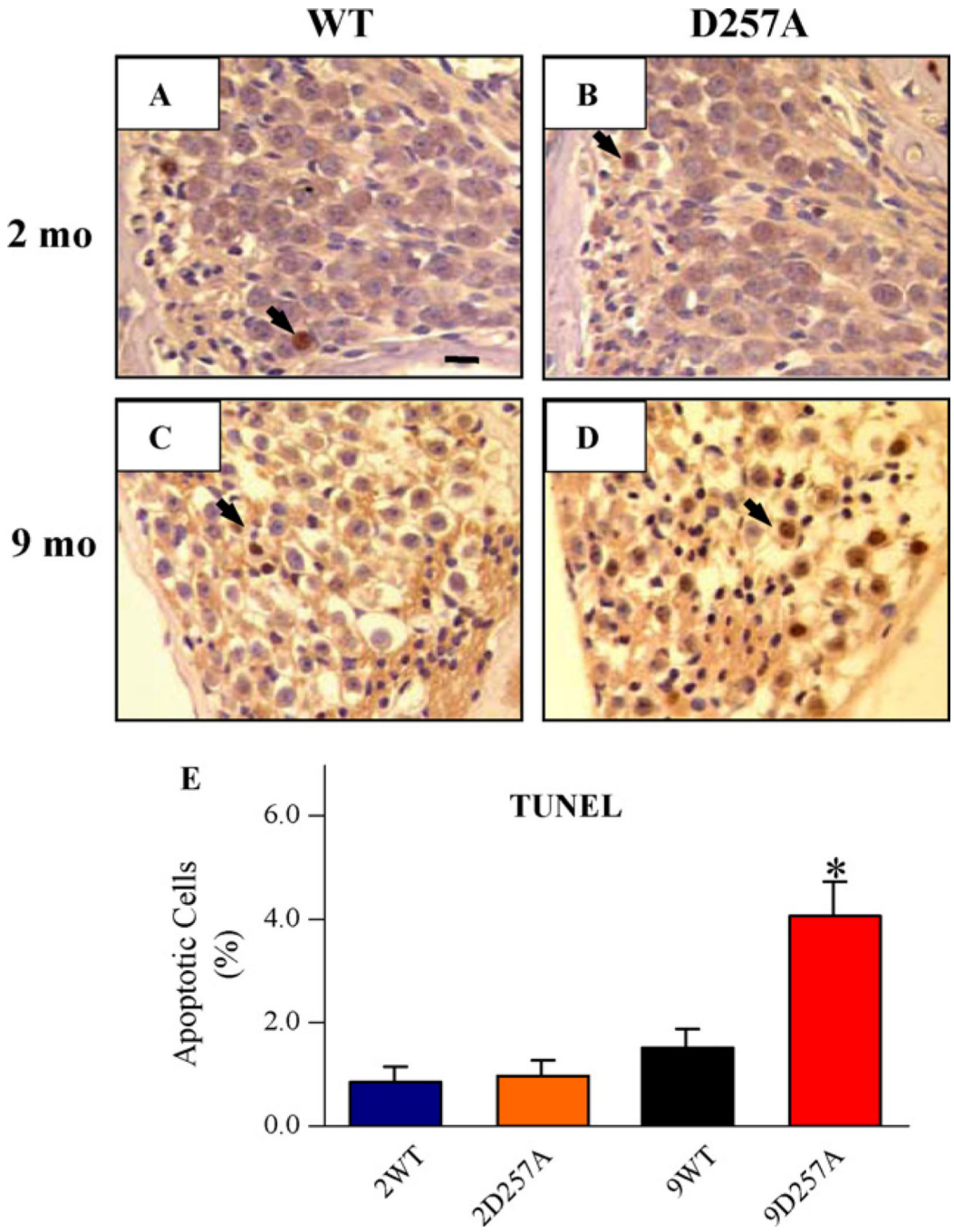

Fig. 5.

Apoptosis detection by TUNEL staining. Detection and quantification of DNA fragmentation in the cochlear apical turn from 2- and 9-month-oldWTand D257A (A–D) mice. Arrows indicate TUNEL-positive staining cells. The cochleae from 9-month-old D257A mice displayed significantly more TUNEL-positive cells relative to those of age-matched WT (E) (*$P < 0.05$, $n = 5$). Error bars represent S.E.M. Scale bar = 25μm.

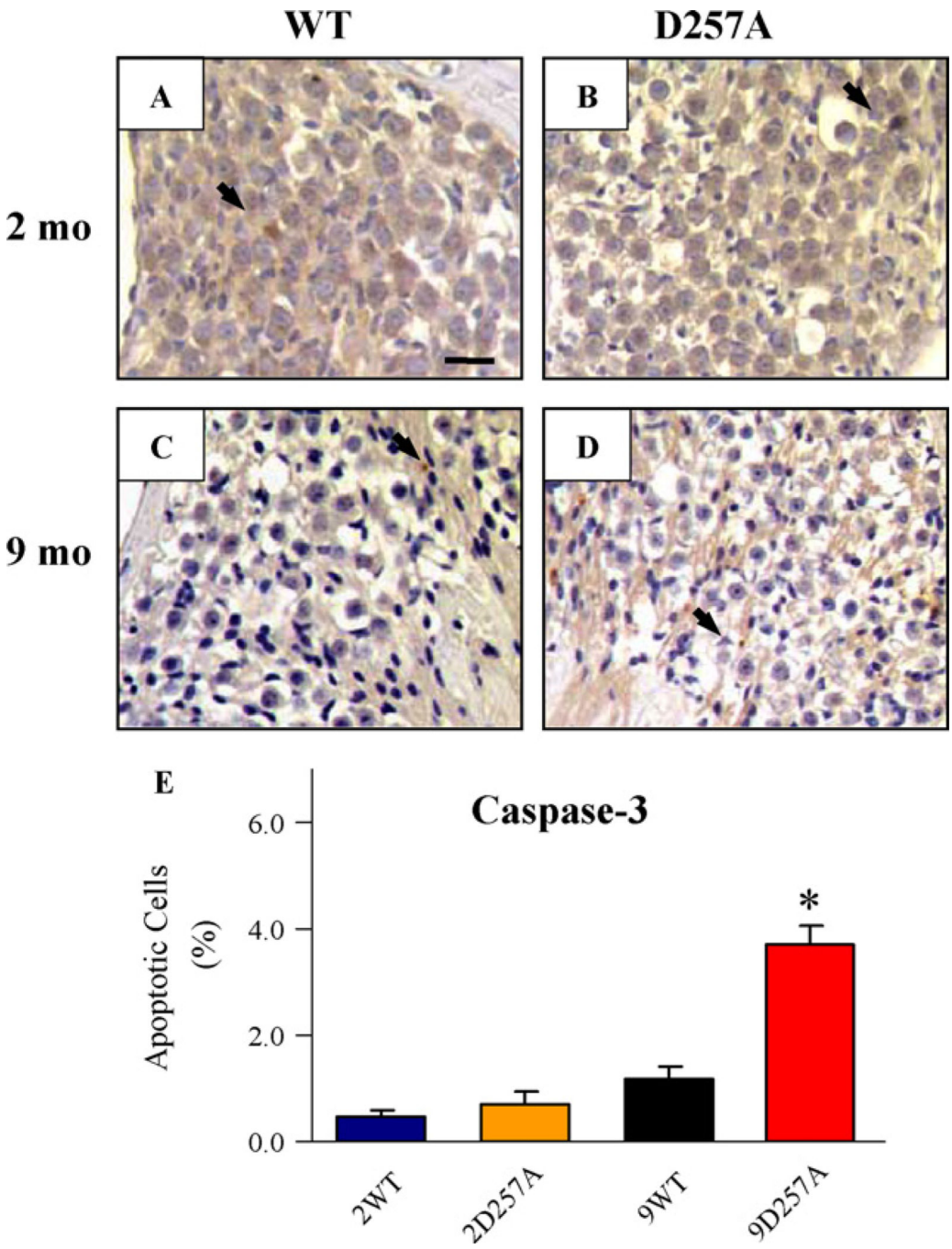

Fig. 6.

Apoptosis detection by active caspase-3 staining. Detection and quantification of cleaved caspase-3 in the cochlear apical turn from 2- and 9- month-oldWTand D257A (A–D) mice by immunostaining. Arrows indicate cleaved caspase-3-positive staining cells. The cochleae from 9-month-old D257A mice displayed significantly more cleaved caspase-3-positive cells relative to those of age-matched WT (E) (*$P < 0.05$, $n = 5$). Error bars represent S.E.M. Scale bar = 25μm.

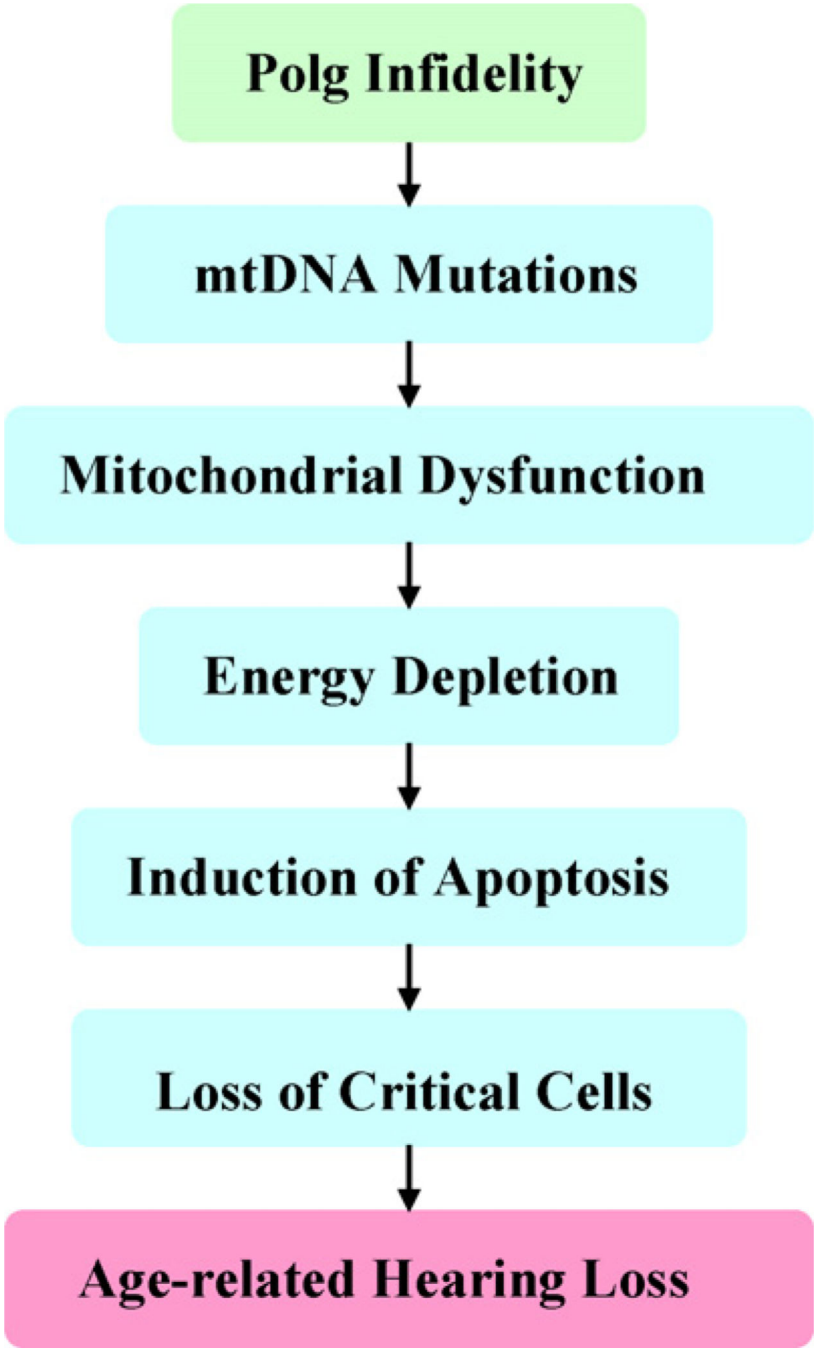

Fig. 7.

Model of how mtDNA mutations impact cochlear function. In this model, a*Polg* mutation causes accumulation ofmtDNAmutations, leading to mitochondrial dysfunction and associated impairment of energy metabolism. The energy depletion in turn induces apoptosis, leading to loss of critical cochlear cells such as hair cells and spiral ganglion neurons. These processes eventually cause loss of cochlear function, resulting in age-related hearing loss.

Table 1

List of “GO: Biological Process” categories of genes significantly associated with mtDNA mutation-responsive genes in the aging cochlea

Biological process categories	N	TN	Fisher
Up-regulated (466 classified genes)			
Ribonucleoprotein complex	23	242	0.000
Ribosome	14	147	0.003
RNA binding	21	285	0.005
Protein binding	71	1401	0.020
Anti-apoptosis	5	41	0.023
Regulation of apoptosis	10	123	0.025
Intracellular transport	25	423	0.031
Down-regulated (378 classified genes)			
Cytoskeleton	39	440	0.000
Extracellular matrix	25	237	0.000
Collagen	8	32	0.000
Structural molecule activity	32	456	0.000
Cell motility	15	158	0.000
Calcium ion binding	28	421	0.000
Myosin	6	33	0.001
Cell adhesion	22	425	0.017
Carbohydrate metabolism	13	239	0.044

N: the number of identified genes in the category; FC: fold change; TN: the total number of genes in the category represented on the GeneChip; Fisher: Fisher Exact test score.

Table 2

List of selected genes significantly associated with mtDNA mutations

Gene ID	FC	*P*-value	FDR	Symbol
Regulation of apoptosis (10)				
BB831420	1.69	0.000	2.9	Gsk3b
AA214868	2.07	0.000	3.2	Pten
BM120925	1.66	0.000	4.0	Bim
NM 007566	1.37	0.001	4.1	Birc6
AF201288	1.11	0.003	6.2	Tsc22d3
BB768208	1.25	0.004	6.6	Sgk3
AB012278	1.35	0.006	7.5	Cebpb
NM 026810	1.23	0.009	8.9	Mlh1
AK011828	1.66	0.010	8.9	Hip1
AF353993	1.32	0.013	9.7	Bbp
Programmed cell death (13)				
NM 011361	1.56	0.000	3.8	Sgk
BC026823	1.39	0.002	5.6	Pdcd6ip
L26349	1.26	0.003	5.9	Tnfrsf1a
Proteolysis and peptidolysis (14)				
BB443585	2.37	0.002	5.4	Adamts4
AK008695	1.63	0.004	6.2	2210010C04Rik
NM 022022	1.08	0.005	6.6	Ube4b
AK020649	1.45	0.005	6.9	Adam 15
BB131619	1.62	0.006	7.5	Lnx1
NM 007800	2.27	0.007	8.2	Ctsg
AK013777	2.42	0.008	8.2	Ptpn21
NM 008585	1.55	0.008	8.2	Mep1a
NM 133216	1.28	0.011	8.9	Xpnpep1
BC013654	1.56	0.011	8.9	Trfr2
Response to stress (15)				
AF047377	1.42	0.002	5.0	Hspb1
BF466143	2.23	0.003	5.9	Wasl
BM234360	1.54	0.003	5.9	Fn1
L77884	2.62	0.003	5.9	Lyst
NM 011558	2.27	0.004	6.6	Tcrg-V4
BB298208	3.39	0.005	6.6	Chek1
BB075261	1.48	0.005	6.9	Fcgr1
NM 016928	1.64	0.006	7.5	Tlr5
NM 011728	1.46	0.007	8.2	Xpa
NM 010824	2.01	0.011	8.9	Mpo
Carbohydrate metabolism (13)				
BQ176370	−1.47	0.00	2.9	9230112O05Rik

Gene ID	FC	*P*-value	FDR	Symbol
NM 008063	−1.29	0.000	4.0	Slc37a4
NM 008832	−1.83	0.001	5.0	Phka1
AW208566	−4.83	0.001	5.0	Lyzs
BG073164	−1.42	0.002	6.2	Pgm2l1
NM 007933	−5.77	0.003	6.9	Eno3
BI685536	−1.35	0.004	7.5	B4galt6
NM 008062	−1.34	0.004	7.5	G6pdx
AK007262	−1.57	0.004	8.2	1700124B08Rik
NM 011079	−3.91	0.004	8.2	Phkg
Mitochondrion (13)				
BC008518	−1.16	0.000	3.8	Nnt
NM 007702	−2.69	0.000	4.0	Cidea
AB022340	−4.11	0.001	4.5	Acsm3
AV278574	−1.42	0.001	5.4	Aldh6a1
NM 007472	−1.65	0.002	6.2	Aqp1
NM 080575	−1.57	0.003	6.9	Acas2l
NM 026331	−1.89	0.004	7.5	Mscp
NM 022032	−1.49	0.004	7.5	Perp
AK017491	−1.47	0.004	8.2	Mipep
BG866501	−1.38	0.005	8.9	Hadhb
Cytoskeleton (39)				
BG094386	−1.27	0.000	2.9	Dag1
BQ032637	−1.49	0.000	3.8	Jak1
BC021484	−1.70	0.000	3.8	Sspn
AK003186	−1.98	0.000	4.0	Tpm2
AF237628	−38.21	0.000	4.0	Lmod2
AK003182	−7.87	0.000	4.0	Myl1
AJ002522	−8.77	0.001	5.0	My h1
NM 010861	−3.49	0.002	6.2	Myl2
BC008538	−136.05	0.003	6.2	Myh2
NM 016754	−6.87	0.005	8.2	Mylpf
Extracellular matrix (25)				
AW550625	−1.91	0.000	2.9	Col3a1
BF227507	−2.95	0.000	2.9	Col1a2
NM 008610	−1.74	0.000	3.8	Mmp2
BC019502	−1.71	0.000	3.8	Bgn
AV229424	−1.58	0.000	4.0	Col5a2
BF158638	−1.35	0.001	5.4	Col4a1
NM 007732	−14.01	0.002	5.6	Col1 7a 1
AF011450	−1.30	0.003	6.6	Col15a1
AF064749	−1.33	0.003	6.6	Col6a3
U08020	−3.18	0.004	7.5	Col1a1

Gene ID	FC	*P*-value	FDR	Symbol
Cell adhesion (22)				
BE199556	−1.43	0.000	3.8	Pard3
AF038562	−5.52	0.000	3.8	Lgals7
NM 009675	−2.53	0.000	3.8	Aoc3
BI110565	−2.01	0.000	4.0	Postn
BB776961	−1.33	0.001	4.5	Cdh13
NM 019759	−2.14	0.002	5.6	Dpt
BB534670	−2.31	0.003	6.9	Cd36
NM 11582	−2.92	0.004	6.9	Thbs4
BQ175493	−1.56	0.004	7.5	Itga8
NM 016685	−2.35	0.007	9.7	Comp
Perception of sound (6)				
BI143915	−1.69	0.001	4.3	Ntn1*
BQ176524	−1.72	0.001	5.4	Bsn*
U08020	−3.18	0.004	7.5	Col1a1*
BQ175493	−1.56	0.004	7.5	Itga8*
NM 010081	−6.85	0.006	8.9	Dst*
NM 013624	−1.52	0.007	9.7	Otog
Ion transport (12)				
BG791642	−1.73	0.001	4.4	Abcc9
BE945884	−2.61	0.001	5.0	Gabra1
BQ175666	−1.55	0.001	5.4	Gabrb3
NM 013540	−2.04	0.004	6.9	Gria2
BB515151	−1.39	0.005	8.2	Tcn2
BM119753	−1.51	0.006	9.7	Kcna6
AF089751	−1.49	0.006	9.7	P2rx4
BB236747	−1.48	0.006	9.7	Clic5
BI650739	−1.33	0.007	9.7	Ubl4
NM 08557	−1.57	0.007	9.7	Fxyd3

Gene ID: representative public gene ID; FC: fold change; *P*-value: *P*-values for the comparison of 9-month-oldWTvs. 9-month-old D257A group; FDR: false discovery rate; symbol: gene symbol.